Bull. Mater. Sci., Vol. 38, No. 4, August 2015, pp. 887–893. © Indian Academy of Sciences.

Sol–gel synthesis of palladium nanoparticles supported on reduced graphene oxide: an active electrocatalyst for hydrogen evolution reaction

FERESHTEH CHEKIN*
Young Researchers and Elite Club, Ayatollah Amoli Branch, Islamic Azad University, Amol 678, Iran

MS received 30 November 2014; accepted 16 March 2015

Abstract. **In this work, the synthesis and characterization of palladium nanoparticle-reduced graphene oxide hybrid (Pd–rGO) material is reported. Techniques of X-ray diffraction, transmission electron microscope (TEM), energy-dispersive X-ray, FT-IR spectroscopy, thermogravimetric analysis and cyclic voltammetry were used to characterize the structure and properties of the Pd–rGO. Results demonstrate the effect of Pd on the reduced GO. The average particle size of the Pd nanoparticles supported on rGO obtained from TEM is about 12–18 nm. Moreover, glassy carbon electrode (GCE) modified with palladium nanoparticle–graphene oxide hybrid (Pd–rGO/GCE) was prepared by casting of the Pd–rGO solution on GCE. The electrochemical and catalytic activity of the Pd–rGO/GCE was studied in 0.1 M H_2SO_4 solution. The Pd–rGO/GCE electrode exhibited remarkable electrocatalytic activity for the hydrogen evolution reaction (HER). At potential more negative than −0.4 V *vs.* Ag|AgCl|KCl_{3M}, the current is mainly due to hydrogen evolution reaction. Finally, the kinetic parameters of hydrogen evolution reaction are also discussed on the Pd–rGO/GCE.**

Keywords. **Reduced graphene oxide; palladium nanoparticles; hybrid; hydrogen evolution reaction.**

1. Introduction

Already various applications utilizing graphene-based material have been reported such as transparent electrodes in solar cells,[1–3] catalytic electrodes in fuel cells,[4] supercapacitors[5,6] as well as electrodes in transistors[7] and sensors.[8] Due to its low catalytic activity, graphene is often decorated with catalytic nanoparticles or quantum dots for applications in fuel cells or optoelectronics,[9] respectively, resulting in hybrid material with both advantages of graphene and nanoparticles often inducing novel properties. For example, platinum or titanium dioxide nanoparticles have high specific surface area and catalytic activity; they have been proven for applications in catalysis[10,11] and for energy conversion.[12,13] Also, semiconducting CdSe nanocrystals (NCs) with easily tunable optical and electrical properties have been demonstrated successfully for application in hybrid photovoltaic devices.[14,15]

However, the nanoparticles are often synthesized in solution with ligand shells to prevent aggregation; this in turn decreases the effectiveness of catalysis or charge transfer in fuel cells and solar cells.[16] This general problem can be overcome by using a framework to support the nanoparticles, keeping them separated and avoiding aggregation. Graphene is an excellent framework and support for nanoparticles.[17,18] Additionally it favours charge transfer processes at the nanoparticle–graphene interface[9] as well as charge transport processes making them ideal candidates for interlayer or electrode material in electrocatalysis or photovoltaic.[19,20]

Taking advantages of the high electrical conductivity, the ultra-high specific area of graphene[8] and good catalytic or optoelectric properties of nanoparticles, the obtained nanoparticle–graphene hybrid materials have high potential in energy harvesting applications. So far, much effort has been paid to the synthesis and application of graphene–metal nanoparticle hybrid material. Platinum or silver nanoparticle decorated graphene was successfully synthesized and exhibits highly catalytic behaviour towards methanol and ethanol oxidation and oxygen reduction as electrode material in fuel cells.[17,18] Another example is CdSe NCs decorated graphene with promising properties for applications in photovoltaics.[9,21–23]

The hydrogen evolution reaction (HER) is an electrochemical process that has received wide attention because of its importance in both fundamental and technological electrochemistry such as fuel cell technology.[24–27] For development of the hydrogen-based fuel cell systems as power sources for emission-free electric vehicles, preparation of an active electrocatalyst is still the main subject. The nature of the electrocatalytic surface plays a decisive role in the kinetics and mechanism of this reaction. Although Pt and Pd present the highest activity for the HER, the high cost of this material is often very prohibitive. The search for new and less expensive alternative material for HER has been a topic of current interest.[28–35] Deposition of Pt or Pd particles on the less expensive material such as carbon supports reduced the cost of anode materials in the industrial applications.

In the present article, we introduce a simple method towards functionalization of graphene oxide with Pd nanoparticles.

*Author for correspondence (fchekin@yahoo.com)

The obtained Pd–graphene oxide was characterized using transmission electron microscopy (TEM), X-ray diffraction (XRD), energy-dispersive X-ray (EDAX), FT-IR spectroscopy and thermogravimetric analysis (TGA). The HER was studied in sulphuric acid solution on glassy carbon electrode (GCE) modified with Pd–rGO as a low cost electrocatalyst.

2. Experimental

2.1 *Materials and apparatus*

Graphite flakes were purchased from Asbury Graphite Mills, Inc. (Asbury, NJ). All the reagents like HCl (AR: 37.5%), H_2SO_4 (AR: 98%), H_2O_2 (AR: 30%) and H_3PO_4 (AR: 60%) were obtained from Fluka Chemicals (Germany). Potassium permanganate was purchased from Tianjin Jiangtian Chemical Reagent Co. Ltd. in China. Gelatin was obtained from Beijing Aoboxing Universeen Bio-Tech Co. Ltd. (Beijing, China). Palladium nitrate was purchased from Aldrich. All other chemicals were analytical grade and were used as purchased.

Electrochemical measurements were performed with an Autolab Potentiostat/Galvanostat (Netherlands). The three-electrode system consists of a Pd–rGO/GCE as working electrode, $Ag|AgCl|KCl_{3M}$ as the reference electrode and a platinum wire as an auxiliary electrode (Metrohm) were used in all voltammetric experiments. LEO-Libra 120 microscope was employed for Pd–rGO transmission electron microscopy images. Fourier transform infrared spectroscopy studies were carried out with BRUKER FT-IR spectrometer. Hitachi S-3500N SEM with electron diffraction and EDAX analysis was used for chemical characterization of a specimen. The crystallization and purity of the synthesized samples were characterized by XRD. The TGA was carried with Mettler Toledo TGA/SDTA 851e.

2.2 *Preparation of Pd–rGO hybrid*

Graphene oxide was fabricated based on the modified Hammer's method.[36] In a typical procedure, about 20 mg of GO was loaded in a 250-ml round bottom flask and 100 ml of distilled water was then added, yielding an inhomogeneous yellowish-brown dispersion. The gelatin was prepared separately by adding 2 g of gelatin crystal in 100 ml of distilled water using hot plate stirrer for maintaining the temperature of 80°C for 30 min to complete dissolution. After that, the pale yellow coloured gelatin solution was added dropwise to yellowish-brown coloured GO dispersion at 80°C using same hot plate stirrer for complete addition. Briefly, 10 ml palladium nitrate solution (1 M) was added to the above solution with continuous stirring. This mixture was allowed to stir for 20 h at 95°C using hot plate stirrer formed blackish gel. Finally, the resulting blackish gel was mixed with small amount of hot water and centrifuged at 7000 rpm for 30 min followed by washing with hot water three times to remove excess gelatin and nitrate. The obtained solid product of Pd–rGO hybrid was redispersed in distilled water (1 mg ml^{-1}) and stored at 4°C for further application.

2.3 *Fabrication of Pd–rGO/GCE*

The dispersed solution of Pd–rGO hybrid was sonicated for 20 min. Finally, a high dispersed solution was formed. Prior to use, the GCE (diameter 1.8 mm) was first polished with alumina (0.05 μm) slurry and ultrasonically cleaned with ethanol and double distilled water then dried in room temperature. Briefly, 5 μl of Pd–rGO hybrid solution was coated on the GCE surface and dried in air.

3. Results and discussion

Figure 1 displays XRD pattern of the rGO and Pd–rGO hybrid. The Pd–rGO sample shows a broad peak at approximately $2\theta = 11°$ corresponding to the (002) reflection of rGO. The Pd loaded on rGO surface nearly has no influence on rGO structure. Pd phase has not been detected in the XRD patterns of Pd–rGO powders, possibly because the Pd content on rGO surface is not enough to form clearly crystalline or Pd is an amorphous phase.

Figure 2 displays TEM image of the rGO and Pd–rGO hybrid catalysts. The TEM image shows the presence of uniform well-dispersed Pd nanoparticles on rGO sheet. From TEM image, we can estimate the average particle sizes of

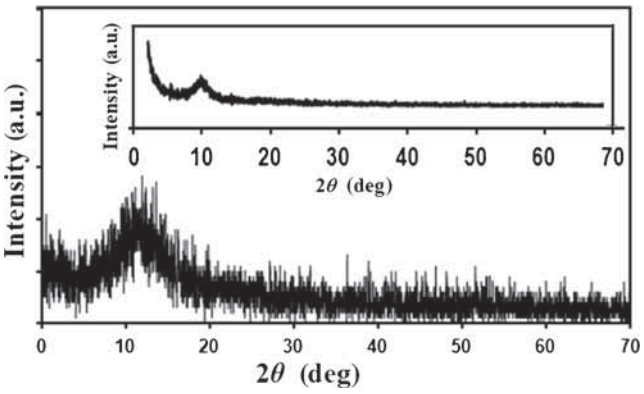

Figure 1. XRD pattern of Pd–rGO hybrid. Inset: XRD pattern of rGO.

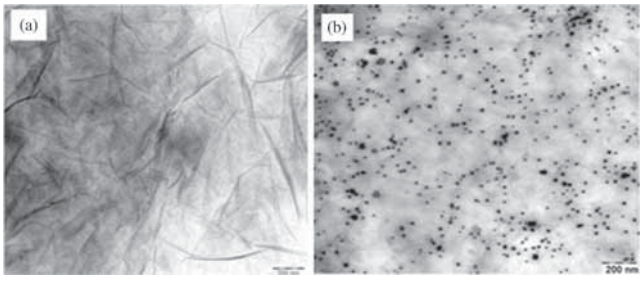

Figure 2. TEM image of (**a**) rGO and (**b**) Pd–rGO hybrid.

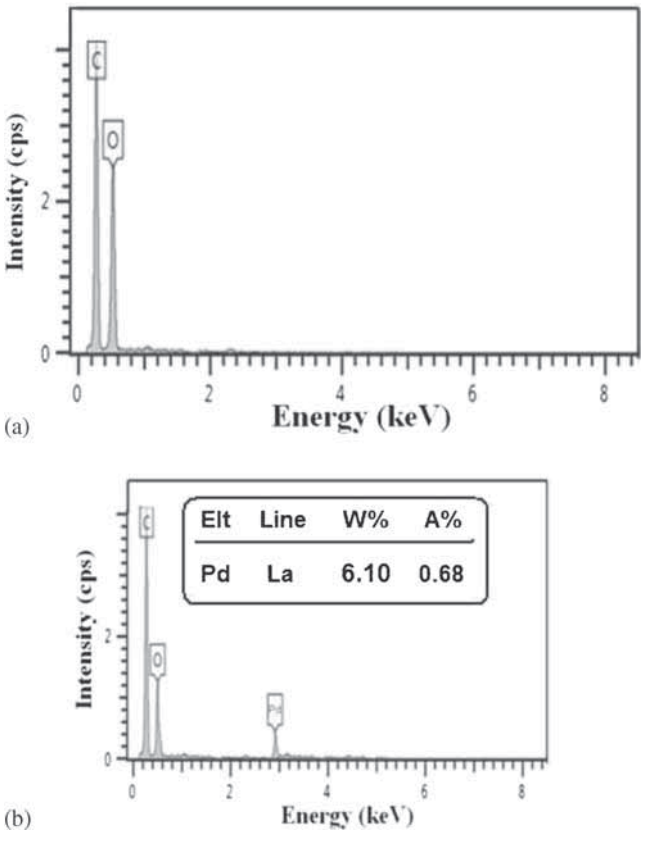

Figure 3. EDAX pattern of (**a**) rGO and (**b**) Pd–rGO hybrid.

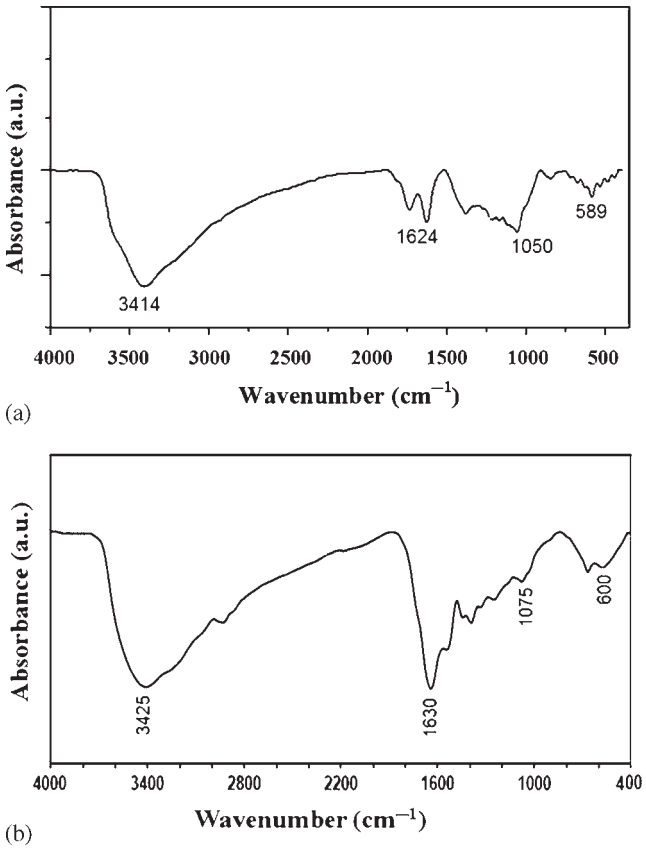

Figure 4. FT-IR spectra of (**a**) rGO and (**b**) Pd–rGO hybrid .

the Pd nanoparticles supported on rGO to range 12–18 nm. It also appears that there are some agglomerations of the Pd nanoparticles on rGO in the range of 20–35 nm.

EDAX analysis (figure 3) clearly shows the presence of Pd (6.1%) in the sample and that the sample consists mainly of carbon with amount of oxygen probably due to the presence of unreduced oxygen functional groups.

The decoration of the surface of the graphene sheets by palladium nanoparticles was discussed by FT-IR spectroscopy. FT-IR spectrum (figure 4) revealed that the resultant Pd–rGO hybrid contained several functional groups like –OH (3425 cm^{-1}), C–O (1075 cm^{-1}) and C=O (1630 cm^{-1}). Therefore it has a strong tendency to readily interact with metal ions by hydroxyl and carboxyl group. A peak at 600 cm^{-1} was signified the formation of Pd–O bond. It is well recognized that the Pd–rGO bonding can be formed through some physic/chemical interactions such as Vander Waals force, H-bonding and other bonds. Pd atoms may possibly react with the –OH and –COOH groups on the functionalized rGO and thus the bonding C–O–Pd or O=C–O–Pd might form through a dehydration reaction.

We have examined the thermal stability of the prepared rGO and Pd–rGO a nitrogen atmosphere using TGA. As shown in figure 5, the Pd–rGO loses its weight in two steps. The first step is at 100°C revealing the evaporation of surface adsorbed water molecules. Second step of weight loss appeared in 200°C suggesting the decomposition of labile oxygen (CO, CO_2, COOH and H_2O vapours) containing

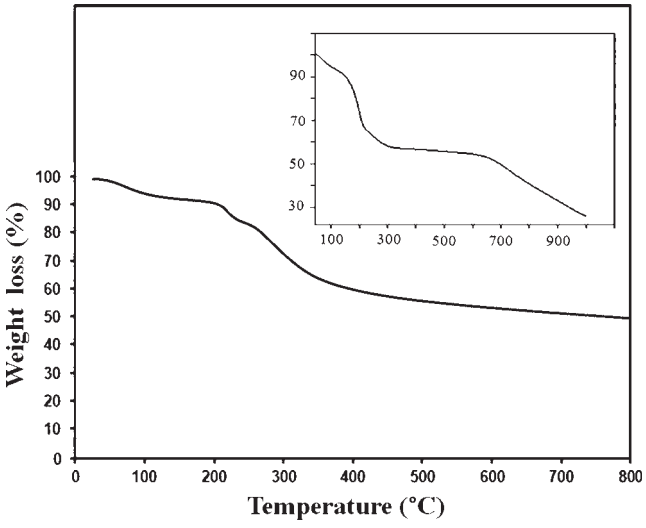

Figure 5. TGA curve of Pd–rGO hybrid. Inset: TGA curve of rGO.

functional groups of rGO. The Pd–rGO catalyst shows high thermal stability. The TGA data also suggest that the presence of Pd nanoparticles on the reduced graphene sheets increases the thermal stability of the Pd–rGO catalyst. However, the mechanism of increasing the thermal stability of graphene by the Pd nanoparticles is not clearly explained at this point. A comparison of particle size, temperature and

Table 1. Compared parameters of synthesized Pd–rGO catalyst with different materials.

Mediator	Method	Agent	Particle size (nm)	Synthesized temperature (°C)	Reference
Pd/Fe_3O_4/graphene	Solvothermal	$FeCl_3$	25	130	37
Pd/graphene oxide	Microwave	Hydrazin	14	150	38
Pd–TiO_2	Sputtering	—	23	900	39
Pd–TiO_2	Electrospinning	Polyvinyl pyrrolidone	25	600	40
Pd–TiO_2	Sol–gel	—	30	500	41
Pd/carbon nanotubes	Chemical	$NaBH_4$	5–20	335	42
Au@Pd	Chemical	Ascorbic acid	11–33	90	43
Pd	Chemical	$NaBH_4$	130	25	44
Pd	Electrochemical	—	50–150	25	45
Pd–rGO	Sol–gel	Gelatin	15	95	This work

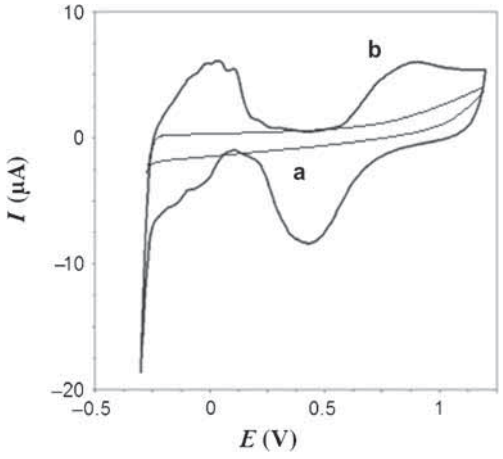

Figure 6. Cyclic voltammogram of (**a**) rGO/GCE and (**b**) Pd–rGO/GCE in 0.1 M H_2SO_4 at a scan rate of 5 mV s^{-1}.

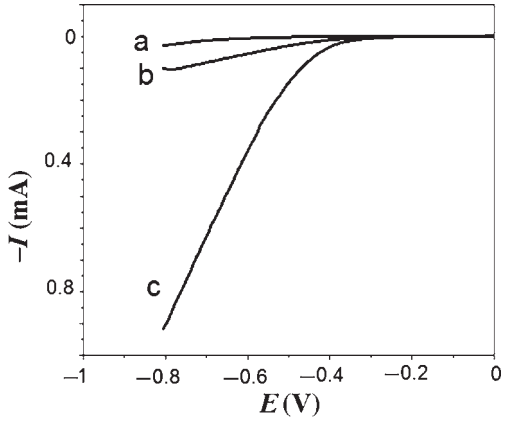

Figure 7. Linear sweep voltammograms of (**a**) bare GCE, (**b**) rGO/GCE and (**c**) Pd–rGO/GCE in 0.1 M H_2SO_4 at a scan rate of 5 mV s^{-1}.

synthesis method of Pd–rGO catalyst synthesized in this work with those already reported[37–45] in literatures is shown in table 1. As shown, parameters are comparable with other results.

To evaluate the electrochemical activity of rGO and Pd–rGO hybrid, cyclic voltammograms experiments were tested within a potential range from −0.3 to 1.2 V at a scanning rate of 50 mV s^{-1} in the solution of 0.1 M H_2SO_4. As seen from figure 6, the Pd–rGO film deposited on a GCE was electrochemically active in which hydrogen adsorption characteristics were presented. The electrochemically active surface area (ECSA) was estimated by integrating the voltammograms corresponding to charge of H^+ adsorption, Q_H (Q_H = 0.0125 μC), from the electrode surface assuming that a monolayer of hydrogen corresponds to an adsorption charge of 210 μC m^{-2} by employing the equation:[46,47]

$$\text{ECSA}\ [\text{m}^2\ \text{g}^{-1}\text{of Pd}] = Q_H\ [\mu\text{C m}^{-2}]/(210\ [\mu\text{C m}^{-2}] \times \text{electrode loading}\ [\text{m}^2\ \text{g}^{-1}\ \text{Pd}]).$$

The ECSA for the Pd–rGO hybrid was estimated to be 11.9 m^2 g^{-1} Pd, and the high ECSA was because of high theoretical specific surface area of graphene as a two-dimensional (2D) nanomaterial that allows easy deposition of the metal catalyst. This is due to the presence of 2D flat planes and oxygen-containing groups.

To evaluate the activity of the Pd–rGO catalyst, the electrocatalysis of HER was studied by linear sweep voltammetry, and results are shown in figure 7. As expected, the electrocatalytic activity improves at surface of Pd–rGO/GCE (surface area = 0.057 cm^2, curve c) as though the onset potential of HER occurs at about −0.4 V *vs.* Ag|AgCl|KCl_{3M} and is indicated by an abrupt increase of the cathodic current. Also, the experiment concerning HER on a bare GCE (surface area = 0.042 cm^2, curve a) and GO/GCE (surface area = 0.025 cm^2, curve b) electrodes was studied as shown in figure 7. As can be seen, at the same current density, the overpotential of HER at Pd–rGO/GCE is lower than that at GCE and GO/GCE.

The onset potential of HER is about −0.38 V for Pd–rGO catalyst, which is comparable with WO_3 nanorods catalyst (−0.4 V), WO_3/C catalyst (0 V), Ni nanowires catalyst (−1.1 V), Pt/Al_2O_3/Al catalyst (−0.35 V), Cu/Pt nanoparticles catalyst (−0.3) and WO_3/carbon nanotube catalyst (−0.65 V).[48–53]

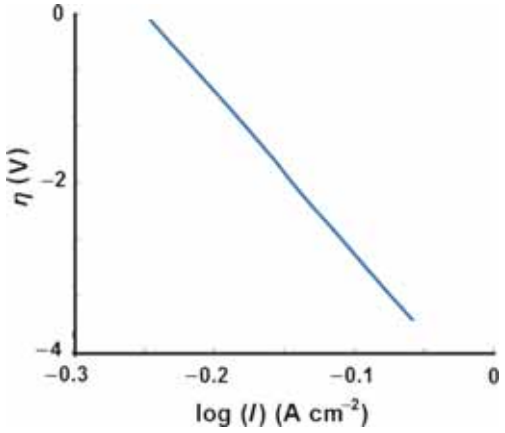

Figure 8. Tafel plot for HER on Pd–rGO/GCE in 0.1 M H_2SO_4 by changing the overpotential values and measure the steady state current of chronoamperometric plots.

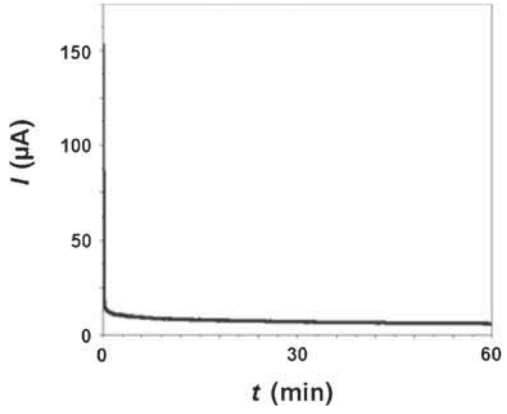

Figure 9. Chronoamperometric curve for Pd–rGO/GCE in 0.1 M H_2SO_4 solution at a fixed potential of −0.5 V.

Tafel plot of Pd–rGO was calculated and transferred from record chronoamperometry plots for a wide potential range by changing the overpotential values and measure the steady state current for each graphs, as shown in figure 8. The Tafel slope for the Pd–rGO electrocatalysts is −122 mV deg^{-1}. The HER mechanism at metal (Me) electrode is based on a 2-step reaction that involves an adsorbed H intermediate, as shown for acidic media below[51]

$$H_3O^+ + 1e^- + Me \rightarrow MeH_{ads} + H_2O \text{ (Volmer step)}, \quad (1)$$

$$MeH_{ads} + H_3O^+ + 1e^- \rightarrow H_2 \uparrow + H_2O + Me \text{ (Heyrovsky step)}, \quad (2)$$

$$2MeH_{ads} \rightarrow H_2 \uparrow + 2Me \text{ (Tafel step)}. \quad (3)$$

The Tafel equation plays an important role in estimating the kinetic mechanism. The Tafel slope is $b = 2.303RT/(\alpha F)$. The charge-transfer coefficient, α, depends on the rate-determining step (rds) for multi-step reactions. The value of α is 0.5 when the rds is Volmer reaction step; the value of α is 1.5 when the rds is Heyrovsky reaction step; the value of α is 2 when the rds is step Tafel reaction.[49] In addition, the Tafel slope $b = 122$ mV deg^{-1} for HER on Pd–rGO/GCE in this work, $\alpha = 1.83$ calculated from $b = 2.303RT/(\alpha F)$. Therefore, Tafel reaction step supposed to be rds for HER on Pd–rGO/GCE.

The Tafel slopes refer to the plots of ln i *vs.* overpotential (η) for HER and the exchange current (i_0) density was derived by extrapolation of the linear part of Tafel plots to zero current potential.

These calculations were made by using the following equation:[54]

$$\eta = (RT/\alpha nF) \ln i_0 - (RT/\alpha nF) \ln i,$$

which is valid at high-overpotential approximation regime. The practical measurement of the electrode activity determinates the overpotential for a constant current density which is 0.60 mA cm^{-2} in our studies, which is higher than for WO_3 nanorods (2.75×10^{-3} mA cm^{-2}), WO_3 black (0.86×10^{-3} mA cm^{-2}), WO_3 supported on carbon black (52.00×10^{-3} mA cm^{-2}), C/CoSn (0.20 mA cm^{-2}), C/CoSnZn (0.70 mA cm^{-2}), C/CoSnZnePd (1.90 mA cm^{-2}), monoclinic WO_3 nanoplates (1.61 mA cm^{-2}), monoclinic WO_3 nanoplates (2.09 mA cm^{-2}), Pd-modified carbon fibre (2.70×10^{-3} mA cm^{-2}) and Pd-modified nickel-coated carbon fibre (1.20 mA cm^{-2}).[48,49,55–57] The high exchange current density of Pd–rGO is implied the lower intrinsic resistance for electronic diffusion in the electrochemical reactions. Throughout from Tafel slope, the number of electron related with hydrogen evolution was also calculated. The number of electrons is 0.76 for Pd–rGO and close to the theoretical number of electrons for HER. Conway and co-workers[58] have shown, by means of Tafel polarization and impedance measurements on several Pt single crystal electrodes, that at low overpotentials the reaction rate of the HER is controlled by the diffusion of H_2 from the surface. At more negative overpotentials, the reaction rate is controlled by the recombination of adsorbed H atoms on the electrode surface. Thus the slope of 122 mV deg^{-1} and α of 1.83, usually determined at wide overpotentials range, Tafel reaction step supposed to be rds for HER on Pd–rGO/GCE.

Finally, the long-term stability of Pd–rGO hybrid modified GC electrode for hydrogen evolution was investigated with chronoamperometric curves recorded at −0.5 V *vs.* $Ag|AgCl|KCl_{3M}$ in 0.1 M H_2SO_4. The result (figure 9) indicated the current does not drop significantly even after 1 h. This result showed that Pd–rGO modified GC electrode had good steady state electrolysis activity for hydrogen evolution in an acidic media.

4. Conclusion

A new route has been developed to prepare Pd–rGO hybrid nanocatalyst. Results of FT-IR, EDAX, TEM, TGA and cyclic voltammetry demonstrate the effect of Pd on the reduced GO. To investigate the catalytic efficiency of Pd–rGO hybrid, the hydrogen evolution reaction was studied

using the deposited film of Pd–rGO hybrid on GCE in 0.1 M H_2SO_4 solution using LSV. The electrocatalytic activity improves at the surface of Pd–rGO/GCE as though the onset potential of HER occurs at about −0.4 V *vs.* $Ag|AgCl|KCl_{3M}$ and is indicated by an abrupt increase of the cathodic current. Pd–rGO hybrid modified GC electrode showed long-term stability for hydrogen evolution in an acidic media.

Acknowledgements

I gratefully acknowledge the financial support by the Young Researchers and Elite Club, Ayatollah Amoli Branch, Islamic Azad University.

References

1. Wang Y, Liu J, Liu L and Sun D 2011 *Nanoscale Res. Lett.* **6** 241
2. Wang H and Hu Y H 2012 *Energy Environ. Sci.* **5** 8182
3. Sahoo N G, Pan Y, Li L and Chan S H 2012 *Adv. Mater.* **24** 4203
4. Xin Y, Liu J G, Zhou Y, Liu W, Gao J, Xie Y, Yin Y and Zou Z 2011 *J. Power Sources* **196** 1012
5. Luan V H, Tien H N, Hoa L T, Hien N T M, Oh E S, Chung J, Kim E J, Choi W M, Kong B S and Hur S H 2013 *J. Mater. Chem. A* **1** 208
6. Li S M, Wang Y S, Yang S Y, Liu C H, Chang K H, Tien H W, Wen N T, Ma C C M and Hu C C 2013 *J. Power Sources* **225** 347
7. Wu Y, Jenkins K A, Valdes-Garcia A, Farmer D B, Zhu Y, Bol A A, Dimitrakopoulos C, Zhu W, Xia F, Avouris P and Lin Y M 2012 *Nano Lett.* **12** 3062
8. Hill E W, Vijayaragahvan A and Novoselov K 2011 *Sens. J. IEEE* **11** 3161
9. Lin Y, Zhang K, Chen W, Liu Y, Geng Z, Zeng J, Pan N, Yan L, Wang X and Hou J G 2010 *ACS Nano* **4** 3033
10. Jin Y, Shen Y and Dong S 2004 *J. Phys. Chem. B* **108** 8142
11. Radhakrishnan C, Lo M K F, Warrier M V, Garcia-Garibay M A and Monbouquette H G 2006 *Langmuir* **22** 5018
12. Plass R, Pelet S, Krueger J and Gratzel M 2002 *J. Phys. Chem. B* **106** 7578
13. Blackburn J L, Selmarten D C and Nozik A J 2003 *J. Phys. Chem. B* **107** 14154
14. Zhou Y, Eck M, Men C, Rauscher F, Niyamakom P, Yilmaz S, Dumsch I, Allard S, Scherf U and Kruger M 2011 *Sol. Energy Mater. Sol. Cells* **95** 3227
15. Ren S, Chang L Y, Lim S K, Zhao J, Smith M, Zhao N, Bulović V, Bawendi M and Gradeĉak S 2011 *Nano Lett.* **11** 3998
16. Ginger D S and Greenham N C 2000 *J. Appl. Phys.* **87** 1361
17. Shang N, Papakonstantinou P, Wang P and Silva S R P 2010 *J. Phys. Chem. C* **37** 15837
18. Qiu J D, Wang G C, Liang R P, Xia X H and Yu H W 2011 *J. Phys. Chem. C* **31** 15639
19. Wang Z, Puls C P, Staley N E, Zhang Y, Todd A, Xu J, Howsare C A, Hollander M J, Robinson J A and Liu Y 2011 *Physica E* **44** 521
20. Gong F, Wang H and Wang Z S 2011 *Phys. Chem. Chem. Phys.* **13** 17676
21. Lu D, Zhang Y, Lin S, Wang L and Wang C 2011 *Analyst* **136** 4447
22. Zedan A F, Sappal S, Moussa S and El-Shall M S 2010 *J. Phys. Chem. C* **114** 19920
23. Wang Y, Yao H B, Wang X H and Yu S H 2010 *J. Mater. Chem.* **21** 562
24. Trasatti S 1991 *Electrochim. Acta* **36** 225
25. Jerkiewicz G and Zolfaghari A 1996 *J. Electrochem. Soc.* **143** 1240
26. Xu Y H, He G R and Wang X L 2003 *Int. J. Hydrogen Energy* **28** 961
27. Christmann K 1988 *Surf. Sci. Rep.* **9** 1
28. Rosalbino F, Delsante S, Borzone G and Angelini E 2007 *J. Alloys Compd.* **429** 270
29. Wu Y M, Li W S, Long X M, Wu F H, Chen H Y, Yan J H *et al* 2005 *J. Power Sources* **144** 338
30. Shibli S M A and Dilimon V S 2007 *Int. J. Hydrogen Energy* **32** 1694
31. Wu M, Shen K P, Wei Z, Song S and Nie M 2007 *J. Power Sources* **166** 310
32. Domınguez-Crespo M A, Plata-Torres M, Torres-Huerta A M, Arce-Estrada E M and Hallen-Lópeza J M 2005 *Mater. Charact.* **55** 83
33. Jafarian M, Azizi O, Gobal F and Mahjani M G 2007 *Int. J. Hydrogen Energy* **32** 1686
34. Karimi Shervedani R and Madram A R 2007 *Electrochim. Acta* **53** 426
35. Xu Y, Chen C, Wang X and Wang Q 2007 *Int. J. Hydrogen Energy* **32** 537
36. Hummers W S and Offeman R E 1958 *J. Am. Chem. Soc.* **80** 1339
37. Chandra S, Bag S, Das P, Bhattacharya D and Pramanik P 2012 *Chem. Phys. Lett.* **519** 59
38. Siamaki A R, Khder A E R S, Abdelsayed V, Samy El-Shall M and Frank Gupton B 2011 *J. Catal.* **279** 163
39. Kim S C, Heo M C and Hahn S H 2005 *J. Kor. Phys. Soc.* **47** 700
40. Moon J, Park Zyung T and Kim D 2010 *Sens. Actuators B* **149** 301
41. Mardare D, Iftimie N, Crişan M, Răileanu M, Yildiz A, Coman T, Pomoni K and Vomvas A 2011 *J. Non-Cryst. Solids* **357** 1774
42. Arrigo R, Wrabetz S, Schuster M E, Wang D, Villa A, Rosenthal D, Girsgdies F, Weinberg G, Prati L, Schlögl R and Su D Sh 2012 *Phys. Chem. Chem. Phys.* **14** 10523
43. Song H M, Moosaa B A and Khashab N M 2012 *J. Mater. Chem.* **22** 15953
44. Mei Y, Lu Y, Polzer F and Ballauff M 2007 *Chem. Mater.* **19** 1062
45. Diculescu V C, Chiorcea-Paquim A M, Corduneanu O and Oliveira-Brett A M 2007 *J. Solid State Electrochem.* **11** 887
46. Li Y, Gao W, Ci L, Wang Ch and Ajayan P M 2010 *Carbon* **48** 1124
47. Chekin F, Bagheri S and Abd Hamid Sh B 2013 *Sens. Actuators B* **177** 898

48. Rajeswari J, Satyananda Kishore P, Viswanathan B and Kanthadai Varadarajan Th 2007 *Nanoscale Res. Lett.* **2** 496
49. Zheng H and Mathe M 2011 *Int. J. Hydrogen Energy* **36** 1960
50. Lee J K, Yi Y, Hye Lee J, Uhm S and Lee J 2009 *Catal. Today* **146** 188
51. Habibi B, Pournaghi-Azar M H, Razmi H and Abdolmohammad-Zadeh H 2008 *Int. J. Hydrogen Energy* **33** 2668
52. Raoof J B, Ojani R, Asghari Esfeden S and Rashid Nadimi S 2010 *Int. J. Hydrogen Energy* **35** 3937
53. Chekin F, Bagheri S and Abd Hamid Sh B 2013 *J. Chin. Chem. Soc.* **60** 447
54. Ojani R, Raoof J B and Hasheminejad E 2013 *Int. J. Hydrogen Energy* **38** 92
55. Jin Ham D, Phuruangrat A, Thongtem S and Sung Lee J 2010 *Chem. Eng. J.* **165** 365
56. Pierozynski B 2013 *Int. J. Hydrogen Energy* **38** 7733
57. Döner A, Tezcan F and Kardas G 2013 *Int. J. Hydrogen Energy* **38** 3881
58. Barber J, Morin S and Conway B E 1998 *J. Electroanal. Chem.* **446** 125